Beta sheet forming peptides functionalization with biologically active motifs may alter their self-assembling propensity

F. Taraballi*, M. Campione**, A. Sassella**, A. L. Vescovi*, W. Hwang***, A. Paleari** and F. Gelain*.

*University of Milan - Bicocca, Bioscence and Biotechnology Department, p.zza della Scienza 2, 20126, Milan, Italy, taraballi@mater.unimib.it, angelo.vescovi@unimib.it, fabrizio.gelain@unimib.it
**University of Milan - Bicocca, Material Science Department, via R.Cozzi 53, 20125, Milan, Italy, marcello.campione@mater.unimib.it, adele.sassella@mater.unimib.it, alberto.paleari@mater.unimib.it
***Texas A&M University - Department of Biomedical Engineering Zachry Engineering Center 337, College Station, TX 77843-3120 (U.S.A.), hwm@tamu.edu

ABSTRACT

Synthetic polymers and bioinspired fibrous materials have a significant impact in medicine in the recent years. The design and fabrication of new bio-materials has a great influence in several scientific and medical communities. The potential benefits to basic science include: understanding of biomolecular self-assembly in water; predicting natural biomolecular assembly from sequence information alone and at least increasing confidence to designing new natural and biomaterials. The "designing rules" of self-assembly are becoming available but not yet completely understood. RADA16-I undergoes molecular self-assembly into double layered β-sheet structures that spontaneously form nanofibers upon exposure to solutions at neutral pH [1]. RADA16-I functionalization with biological active motifs may influence the self-assembling tendency of new functionalized peptides. This explorative study attempts to give different tools to characterize this group of synthetic peptides. Three different functionalized peptides, showing different hydrophobicity profile and local charge, have been analyzed by micro-Raman spectroscopy and Atomic Force Microscopy (AFM). Farther more computational experiments using molecular dynamic (MD) simulations confirm the experimental findings and indicate themselves as good tools to predict the behaviour of these peptides in aqueous solution.

Keywords: functionalized peptides, atomic force microscopy, micro-Raman spectroscopy, molecular dynamic.

1 INTRODUCTION

The self-assembly of peptides or other biopolymers plays an important role in the discovery of new materials and scaffolds, with a wide range of applications in nanotechnology and nanomedicine such as regenerative medicine and drug delivery systems. A class of ionic self-complementary synthetic peptides (usually made of 16 to 30 residues) spontaneously forms hydrogels when exposed to body fluids or, more generally, solutions at physiological pH; for these reasons are suitable for the tissue regeneration.

RADA16-I family peptides spontanueously self-assemble into a double-layered β-sheet [2]. When RADA16-I is functionalized in C-terminal with the bone marrow homing peptide BMHP1 (PFSSTKT) is capable of stimulating neural stem cell adhesion, proliferation and differentiation [3]; when extended with bone-cell secreted signal peptide ALK (ALKRQGRTLYGF) it promotes mouse osteoblasts proliferation and differentiation [4]; while the functionalization with the osteopontin derived peptide sequence SDE (SDESHHSDESDE), a bone ECM molecule regulating cell adhesion, migration and survival, is a FP newly designed for bone regeneration applications never tested before. The different functional motifs significantly influence the FP propensity to self-assemble and the overall mechanical properties of the scaffold at the meso-scale. For a rational functionalization of new self-assembling peptides, it is thus necessary to understand how different functional motifs can affect the self-assembly propensity of the self-assembling "core" sequences. Therefore, we investigate the three functionalized peptides by using a combination of experimental and simulation approaches with the main aim of investigating how functional motifs may influence self-assembling in RADA16-I derived peptides.

2 MATERIALS AND METHODS

2.1 Materials synthesis

RADA16-I solution (1%), commercially available as PuraMatrix was purchased from BD Bioscience, Bedford, MA. The functionalized designer peptides were custom-synthesized with a CEM Liberty Microwave Peptide Synthesizer (Matthews, NC). All FPs were purified by HPLC in CH3CN/Water gradient. They were dissolved in water at a final concentration of 1% (w/v) and sonicated for 20 min prior usage.

2.2 Simulation methods

In simulation experiments, we used CHARMM [5] version 29 with the PARAM19 force field [5]. In all molecular dynamics (MD) simulations the solvation effect was incorporated by using the analytic continuum electrostatics (ACE2) module incorporated in CHARMM. The filament structures were constructed as a β-sheet bi-layer using 15 peptides on each sheet [6]. After building the filament structure, the system was initially energy-minimized for 200 steps of the steepest-descent method, followed by 3000 steps of the adapted-basis Newton-Raphson (ABNR) method. The system was then heated from 0 K to 300 K in 100 ps, and equilibrated for 300 ps. The final production lasted for 1 ns with Leap integration method. Visualization of molecular conformations and MD trajectories was performed using VMD.

2.3 Atomic force microscopy

FPs at a concentration of 1% w/v solution was diluted in a ratio of 1:200 in sterile water and 5 μl of this final solution was placed on a mica muscovite substrate and kept at room temperature for 1 minute. The mica surface was then rinsed with Millipore-filtered water to remove loosely bound protein and dried under a stream of gaseous nitrogen.

AFM images were collected in tapping™ mode by a MultiMode Nanoscope IIIa (Digital Instruments) under dry nitrogen atmosphere using single-beam silicon cantilever probes (Veeco RTESP: resonance frequency 300 KHz, nominal tip radius of curvature 10nm, force constant 40 N/m). The fiber dimensions were corrected because of the convolution effect arising from the finite size of the AFM tip with the formula [7]:

$$\Delta x = \sqrt{2\left[h\left(2r_t - h\right)\right]} \qquad (1)$$

where Δx is the width broadening effect, h is the nanofiber height, and r_t is for tip radius.

The diameter of the globular aggregates has to be corrected with the formula [7]:

$$R = w^2 \Big/ \left(16 r_t\right) \qquad (2)$$

where R is the corrected radius, w is the measured width, and r_t is the tip radius.

2.4 Raman measurements

Raman spectra were collected on dried samples obtained either from water evaporation or 12h treatment in a lyophilizer (Labconco). As the latter procedure gave the best signal-to-noise ratio with no interference from water phonon spectrum it was the most used in the following experiments. No detectable modification of the Raman pattern resulted from water removal. Powder samples were deposited on a silicon wafer. Measurements were carried out using the 632.8 nm line of a He-Ne laser as light source and collecting the scattered light signal in backscattering geometry by a Raman spectrometer (Labram Dilor). The laser was focused on the sample with a spot diameter of about 2 μm. Signal was detected by means of a CCD (Jobin-Yvon Spectrum One 3000), with a spectral resolution of 1 cm^{-1}, by averaging 10 spectra each taken with a 180 s of acquisition time. The background from the silicon Micro-Raman spectrum, although almost negligible in the investigated 900-1800 cm^{-1} spectral range containing the main features of the protein spectra, was subtracted. Spectra were then normalized to the peak at ~970 cm^{-1} from C-C stretching to make the comparison easier.

Proteins vibration mode, amide I band, appears in the 1600-1700 cm^{-1} region of the Raman spectrum. The amide I region was fit with Origin 7. A Gaussian interpolation function was employed.

The region considered in the band fitting procedure goes from 1630 cm^{-1} to 1700 cm^{-1}. The baseline from 1550 cm^{-1} to 1750 cm^{-1} was assumed to be linear. Comparison of the χ^2 values and R^2 value were used as the criteria for assessing the quality of fit.

3 RESULTS

Four different self-assembling peptides, showing various hydrophobic profiles at their added functional motifs, have been analyzed in this work via molecular dynamics in order to predict their self-assembling propensity.

During MD, the three filaments exhibited different conformational behaviors (Figure.1)

For RADA16-I-BMHP1 and RADA16-I-ALK, the β-sheet bilayer structure of the RADA16-I part remain stable even at 450 K during the 1-ns simulation period (Figure 1a,b). RADA16-I-SDE filament split within 1 ns (Figure 1c), likely due to the strong hydrophilic nature of the functional tail added to RADA16-I.

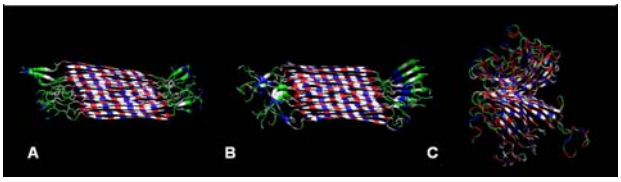

Figure 1. Final conformations of initial double-layered β-sheet structures after 1-ns MD. a) RADA16-I-BMHP1, b) RADA16-I-ALK, c) RADA16-I-SDE. Molecules are visulized via VMD in mode "color for type": blue (basic), white (hydrophobic), red (acidic), and green (polar).

The SDE motif lacks hydrophobic residues, thus shows a tendency to be solvated individually rather than to form a cluster. RADA16-I-BMHP1 and RADA16-I-ALK have hydrophobic residues that drive cluster formation among the added tails. To confirm this virtual results we investigate with AFM and Raman Spectroscopy the structure of each FPs in comparison with RADA16-I.

AFM imaging showed remarkably different nanostructures among the four tested self-assembling peptides (Figure2). RADA16-I forms nanofibers (Figure 2a), as widely described in the previous works [2]. The nanostructure of RADA16-I-BMHP1 (Figure 2c) looks similar to the RADA16-I structure, in spite of an average nanofiber width (14.0±1.6 nm) significantly larger than that one measured for RADA16-I nanofibers (9.4±1.2 nm). The fiber thickness is observed to be multiple of ± 0.5 nm for both materials. The increase of the nanofiber width is expected as the effect of the added functionalized tails flagging from the self-assembled cores. While RADA16-I-ALK molecules make globular structures rather than nanofibers and, as no recurrent lengths of these round-shaped aggregates have been detected, they seem to be non-ordered structures. RADA16-I-SDE (Figure 2d) exposure to PBS did not induce a detectable assembled nanostructure; however, an accurate observation of the sample surface and a comparison with images acquired in the same conditions on the bare mica surface evince that a uniform layer (roughness: 0.2 nm) is formed on the mica surface.

To investigate in details the secondary structure of each FPs we also run Raman measurements of each FPs in the same condition of AFM images.

Information on the secondary structure of peptides may be obtained from the analysis of the amide regions [8]. Particularly, the shape of the amide I band allows to identify contributions from α-helices, β-sheets, and unstructured β–strands. The analysis in Gaussian components shows that this region is satisfactorily reproduced by three main components with spectral position and bandwidth (data not shown). The results of the analysis are consistent with previous works [8] that demonstrated that the band at 1658 cm^{-1} is a marker of alpha-helix, the second band around 1670 cm^{-1} is associated to β-sheet, while the broad band at higher energy is due to unstructured β-strand.

RADA16-I-BMHP1 shows a band shape quite similar to the self-assembling "core", namely RADA16-I. The band is dominated by the narrow peak at 1674 cm^{-1}, ascribable to C=O stretching in β-sheet aggregation, consistently with the formation of fibers observed in AFM images. The band broadening in the amide I region is peculiar of the spectra of RADA16-I-ALK and RADA16-I-SDE and evidences the predominance of conformations dissimilar from β-sheet ones. In fact, the band broadening is different in the two situations, and the intensity ratio between the components at 1655 and 1690 cm^{-1} drastically changes, indicating that the unstructured β-strand conformation is dominant in RADA16-I-SDE, while molecule torsions typical of α-helix structure is favored in RADA16-I-ALK functionalized peptides.

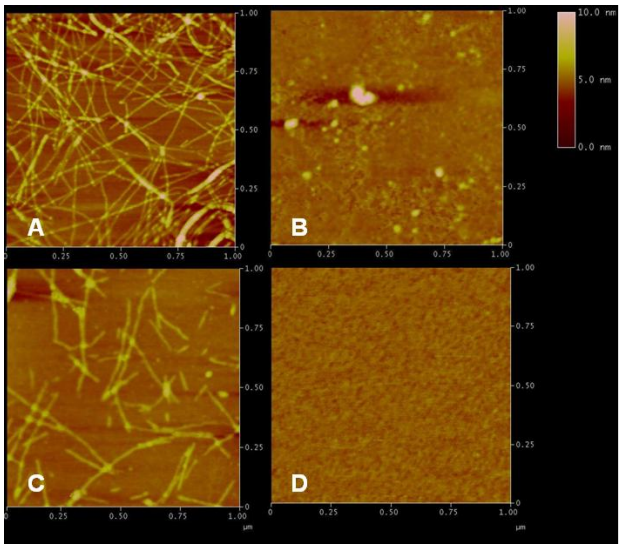

Figure 2. AFM images of FPs at a concentration solution of 1% (w/v). a) RADA16-I self-assembles into nanofibers., b) RADA16-I-ALK aggregates into globular structures. c) RADA16-I-BMHP1 self-organize into nanofibers larger than those shown in (a) d) RADA16-I-SDE evenly coats the mica surface.

There is another interesting spectral region around 1400-1500 cm^{-1}. Specifically, we observed that in this region there is a peak that appear extremely sensitive to self-assembling, showing higher intensity in non-assembled structure, either α-helix or β-strand, than in β-sheet fibers.

4 DISCUSSION

RADA16-I-BMHP1 and RADA16-I-ALK have hydrophobic residues that drive cluster formation among the added tails (Figure 1a, 1b). The balance between hydrophobic and hydrophilic interactions play a relevant role in controlling the aggregation propensity and the aggregate morphology: if the added group is too

hydrophobic, while aggregation is promoted, it is difficult to form an ordered fibril, since it is kinetically easier to form globular aggregates.

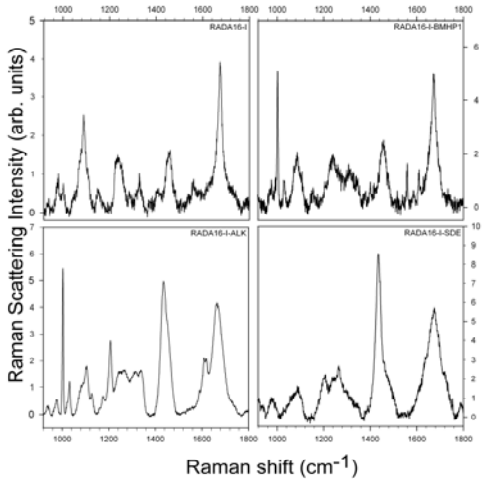

Figure 3. Raman Spectra (900-1800 cm^{-1} region) of the tested self-assembling peptides. Amide I and Amide III peaks are clearly visible (respectively ~1600-1700 cm^{-1} and 1200-1300 cm^{-1}). a) RADA16-I and b) RADA16-I-BMHP1 show similar spectra with the exclusion of the aromatic features given by the Phe c) RADA16-I-ALK and d) RADA16-I-SDE spectra are significantly different from a) and b) in the Amide I region and also for the 1400-1500 cm^{-1}region.

On the other hand, strongly hydrophilic groups prevent aggregation and increase solubility of the peptide. This hypothesis is confirmed by AFM images. The globular shape of RADA16-I-ALK can be explained by the increased hydrophobicity given by the added functional motif. Indeed, as shown by the MD, it is possible to state that the fast kinetic of folding of RADA16-I-ALK cause the globular structure rather than a ordinate fibrillar assembly. Nonetheless RADA16-I-SDE does not arrange itself in a definite structure as indicated by the MD. The scarce self-assembling propensity of this FP is rather expected: ASA calculation (data not shown) shows a high and varying surface area exposed to the solvent. The highly hydrophilic SDE motif added to RADA16-I perturbs the otherwise stable structure of RADA16-I.

Raman data confirm the findings of MD simulations and also give evidence that strong hydrophobic features of RADA16-I-ALK induce the formation of intra-molecular conformations that prevent that the peptide self-assembling in β-sheets; even though, as suggested by the results of molecular dynamics, β-sheet inter-molecular interactions appear to be rather stable once they are formed.

5 CONCLUSIONS

Molecular Dynamics simulations showed a different self-assembling propensity of three FPs with different hydrophobicity profiles. In both MD and in AFM imaging RADA16-I-BMHP1 privilege the double layer β-sheet assembled molecular structure like RADA16-I. On the other hand RADA16-I-SDE shows a marked propensity to open the double-layer initial configuration favoring the solvatation of water to a nanofiber structure.

Raman spectroscopy confirmed AFM findings and the simulations data: it also provided new intriguing possibilities to investigate the self-assembled structure of FPs, new promising biomaterials for tissue engineering, drug delivery and other applications. FP designing requires a better understanding of their nanostructure formation as a consequence of the added functional motifs. These three different investigation techniques may indicate new promising strategies for designing and synthesizing novel functionalized self-assembling biomaterials.

6 REFERENCES

[1] S. Zhang , T. Holmes, C. Lockshin, A. Rich, Proc. Natl. Acad. Sci. U. S. A. 1993, 90, 3334-3338

[2] H. Yokoi, T. Kinoshita, S. Zhang, Proc. Natl. Acad. Sci. U.S.A. 2005, 102, 8414-8419.

[3] F. Gelain, D. Bottai, A. Vescovi, S. Zhang, PLoS ONE 1, 1e119, 2006.

[4] A. Horii, X. Wang, F. Gelain, S. Zhang, PLoS ONE, 2, 2e190, 2007.

[5] B. R. Brooks, R. E. Bruccoleri, B. D. Olafson, D. J. States, S. Swaminathan, M. Karplus, J. Comp. Chem. 1983, 4, 187–217

[6] J. Park, B. Khang, R. D. Kamm, W. Hwang, Biophys. J. 2006, 90, 2510-24.

[7] S. Jun, Y. Hong, H. Imamura , B. Y. Ha, J. Bechhoefer, P. Chen, Biophys. 2004,87, 1249-59.

[8] M. Apetri, N. Maiti, M. Zagorski, P. Carey, V. E. Anderson, J. Mol. Biol. 2006, 355, 63-71.